

Superhard hexagonal transition metal and its carbide and nitride: Os, OsC, and OsN

Jin-Cheng Zheng*

Brookhaven National Laboratory, Upton, New York 11973, USA

and Cavendish Laboratory, University of Cambridge, Madingley Road, Cambridge CB3 0H3, United Kingdom

(Received 18 January 2005; published 8 August 2005)

Recent experimental findings suggest that the bulk modulus of osmium is comparable to that of diamond. From first principles calculations we examine the compressibility of diamond, Os, OsC, OsN, and OsO₂ as well as cubic BN under pressure. We show that Os, OsC, and OsN in the hexagonal structures are less compressible than their cubic phases. The bulk moduli of hexagonal Os, cubic Os, and hexagonal OsC are smaller than that of diamond but larger than cubic BN. Our results indicate that the hexagonal OsC is a promising superhard material.

DOI: 10.1103/PhysRevB.72.052105

PACS number(s): 64.30.+t, 62.20.Dc, 71.15.Mb, 71.20.-b

Although it is long known that diamond is the hardest existing material with the highest known bulk modulus of 443 GPa,¹ there still has been ongoing effort to search another material as hard as or even harder than diamond. Two kinds of materials are believed to be possible superhard candidates. One is the strongly covalent-bonded solids, such as

diamond, cubic boron nitride (*c*-BN), carbon nitrides,² and carbon dioxide.³ The other kind of superhard materials is the transition metals and their carbides, nitrides, and oxides [such as ZrO₂, TiO₂, and HfO₂ (Ref. 4)]. The bulk modulus of solid osmium was measured to be 462 GPa by Cynn *et al.*,⁶ higher than that of diamond [443 GPa (Ref. 1)]. More

TABLE I. The calculated lattice parameters, a_0 (Å), c/a , bulk moduli B_0 (GPa), and their pressure derivatives B'_0 , as well as equilibrium volumes V_0 (Å³/atom) and compared with available experimental data and other computational results.

Materials	Lattice constant a_0 (Å)	c/a	B_0 (GPa)	B'_0	V_0 (Å ³ /atom)
Diamond	3.537		438	3.55	5.530
	3.567 ^f		443, ^c 444 ^e	1–2.5; ^c 4 ^c	5.673
	3.562 ^g		467.1, ^c 446 ^g	3.6, ^c 3.45 ^g	5.505, ^c 5.649 ^g
Os (hex)	2.746	1.578	403	4.36	14.154
		1.580 ^a	462±12 ^a		13.978 ^b
		1.580 ^j	411±6 ^j	4.0±0.2 ^j	13.971, ^j 13.979 ^k
	2.7348(9) ^l	1.5794(6) ^l	395(15) ^l	4.5(5) ^l	13.749 ^c
Os(fcc)	3.845		401	4.15	14.216
	3.83 ^d		419 ^d		
OsC(WC)	2.928	0.928	396	3.97	10.086
	3.592		381	3.49	5.795
<i>c</i> -BN	3.617, ^f 3.610 ^g		369, ⁱ 392 ^g	3.79 ^g	
OsN(WC)	2.743	1.130	367	5.08	10.093
OsC(NaCl)	4.333		366	3.91	10.176
	4.33 ^d		392 ^d		
OsN(NaCl)	4.335		342	4.15	10.185
	4.32 ^d		372 ^d		
OsO₂(rutile)	4.499	0.752	302	3.72	10.748
	4.51 ^h	0.707 ^h			

^aExperiment (Ref. 6).^bExperiment (Ref. 4).^cFP-LMTO(LDA) (Ref. 6).^dPlane wave pseudopotential (LDA) (Ref. 5).^eExperiment (Ref. 1).^fExperiment (Refs. 17 and 18).^gLMTO-ASA(LDA) (Refs. 19 and 20).^hReference 21.ⁱExperiment (Ref. 22.)^jExperiment (Ref. 7).^kCSD (Inorganic Crystal Structure Database) cited in (Ref. 7).^lExperiment (Ref. 8).

TABLE II. The relative energy of cubic Os, OsC, and OsN in comparison with their hexagonal phases (the total energy for the hexagonal phases are set to 0 eV as a reference).

Systems	Os (fcc)	OsC (NaCl)	OsN (NaCl)
Relative energy (eV/atom)	0.075	0.464	0.224

recently, it has been determined to be 411 ± 6 GPa by Ocelli *et al.*⁷ and 395 ± 15 GPa by Kenichi *et al.*⁸ using different experimental methods. These values, although smaller than that of diamond, are still considered to be quite large. The carbides, nitrides and oxides of osmium are therefore expected to be less compressible materials. The bulk moduli of osmium carbide (OsC) and osmium nitride (OsN) in the cubic phases (NaCl structure) have been predicted from first principles calculations to be 392 GPa and 372 GPa, respectively.⁵ However, less studies has been done on the compressibility of the more stable hexagonal structures of OsC and OsN. In this work, *ab initio* pseudopotential total energy calculations are performed to systemically examine the compressibility of Os, OsC, and OsN in both the cubic and hexagonal structures, as well as OsO₂ in the rutile structure.

Calculations on Os, OsC, OsN, and OsO₂ have been performed by the CASTEP code⁹ (version 4.6) using *ab initio* pseudopotentials¹⁰ based on Density Functional Theory (DFT) (Ref. 11) and employing the generalized gradient approximation (GGA-PW91) (Ref. 12) of exchange-correlation effects and Vanderbilt's ultrasoft pseudopotentials.¹³ The cut-off energies are 340 eV for Os, OsC, and OsN, and 380 eV for OsO₂, respectively. For comparison, diamond and *c*-BN are also calculated with cutoff energies of 310 eV and 280 eV, respectively. The special *k*-points are generated using the Monkhorst-Pack scheme¹⁴ with a grid of 0.05 \AA^{-1} .

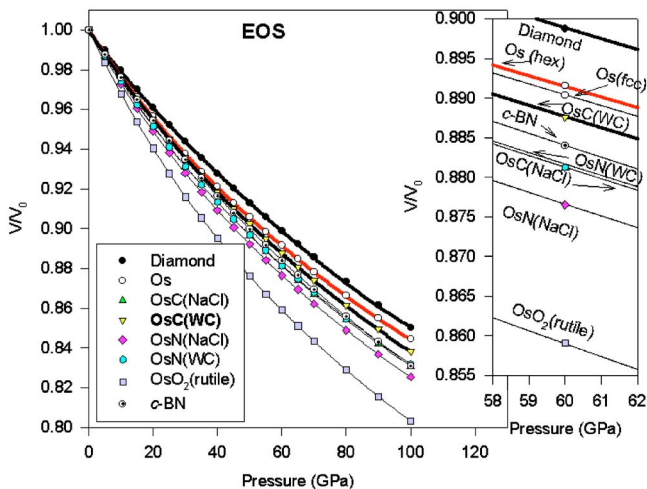


FIG. 1. (Color online) The calculated volume-pressure data (EOS) of diamond, Os, OsC, OsN, OsO₂, and cubic BN. [The EOS near the experimental pressure of 60 GPa is shown in the inset figure, where diamond, Os (hex) and OsC(WC) are highlighted by thicker solid lines.]

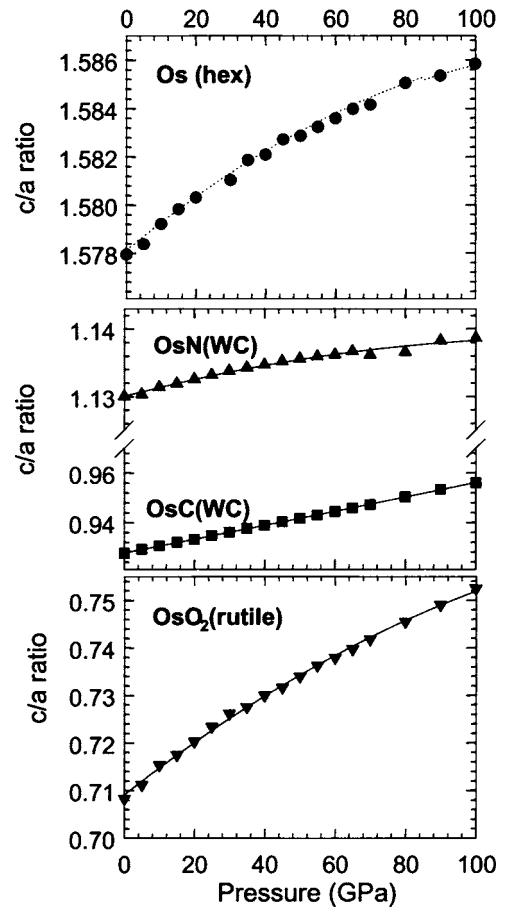


FIG. 2. The calculated *c/a* ratios for Os (hex), OsC(WC), OsN(WC), and OsO₂ (rutile) as a function of pressure.

As shown in Table I, the calculated lattice constant of diamond is 3.537 \AA , which is in good agreement with the experimental value of 3.567 \AA , with an error of 0.84%. The bulk modulus of diamond calculated in this work is 438 GPa, which is underestimated by 1.1% compared with the experimental value of 443 GPa. For the *5d* transition metal, Os, the calculated lattice parameter *c/a* (1.578) and equilibrium volume ($14.154 V_0 \text{ \AA}^3/\text{atom}$) are in good agreement with the experimental values of 1.580 (Ref. 6) [or 1.579 (Ref. 15)] and 13.978 (Ref. 16) [or 13.99 (Ref. 14)], respectively. The bulk modulus (403 GPa) of Os (hexagonal) is smaller than the measured value of 462 ± 12 GPa by Cynn *et al.*,⁶ but agrees well with the recent experimental data 411 ± 6 GPa by Ocelli *et al.*⁷ and 395 ± 15 GPa by Kenichi *et al.*⁸ within the experimental error bars. For comparison, we also calculate Os in the fcc structure⁵ to have a bulk modulus of 401 GPa, which is slightly smaller but still comparable to the one of the hexagonal Os. Our calculations suggest that both phases of Os have low compressibility and high bulk moduli.

OsC and OsN in the NaCl structure have been predicted to be superhard materials with bulk moduli 392 and 372 GPa, respectively,⁵ and our calculations give 366 GPa for OsC and 342 GPa for OsN for the same cubic structure. However, OsC and OsN are more energetically stable in the hexagonal (WC-like) structure under the ambient pressure, as shown in Table II. In the pressure range of 0–100 GPa in

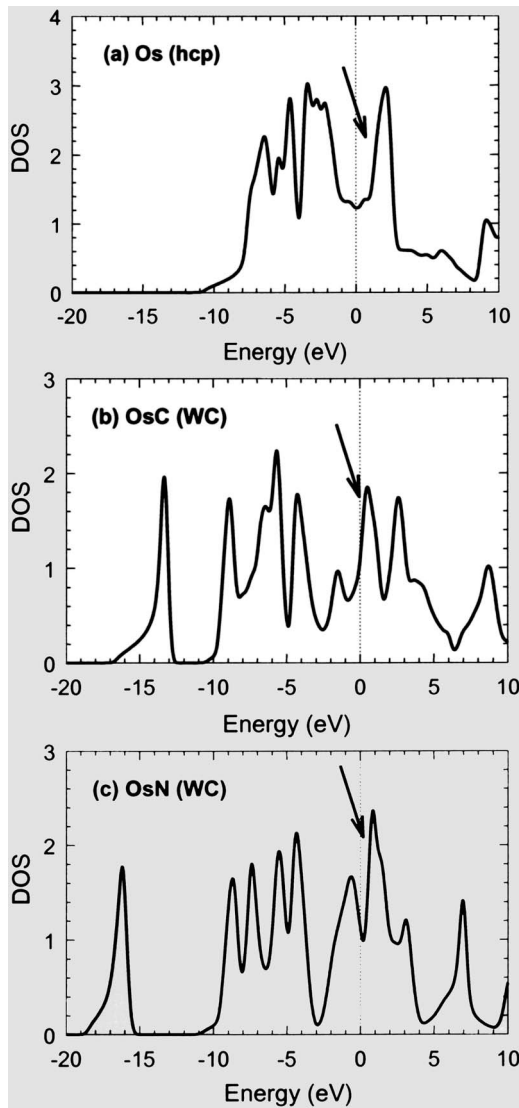


FIG. 3. Total density of states (DOS) of Os (hcp), OsC(WC), and OsN(WC). The arrows indicate the change of antibonding states. Fermi energy is located at 0 eV.

this study, it is found that Os and its carbide and nitride are also energetically favorable in the hexagonal phases. That means the cubic phases can be formed only under the non-equilibrium condition. As shown in Table I, the bulk moduli of the hexagonal OsC (396 GPa) and OsN (367 GPa) are larger than those in the cubic phases. The bulk modulus of osmium oxide (OsO_2) is 302 GPa, smaller than those of osmium carbides and nitrides.

To compare the compressibility of Os and OsC, OsN, OsO_2 under pressure, the volume compressions as a function of pressure are plotted in Fig. 1. The order of compressibility from low to high is: diamond < Os(hex) < Os(fcc) < OsC(WC) < c -BN < OsN(WC) < OsC(NaCl) < OsN(NaCl) < OsO_2 (rutile), as also can be deduced from their bulk moduli listed in Table I. The equation of state (EOS) also shows that OsC in the WC structure has the lowest compressibility among the osmium compounds of osmium carbides, nitrides, and oxide. The dependence of vol-

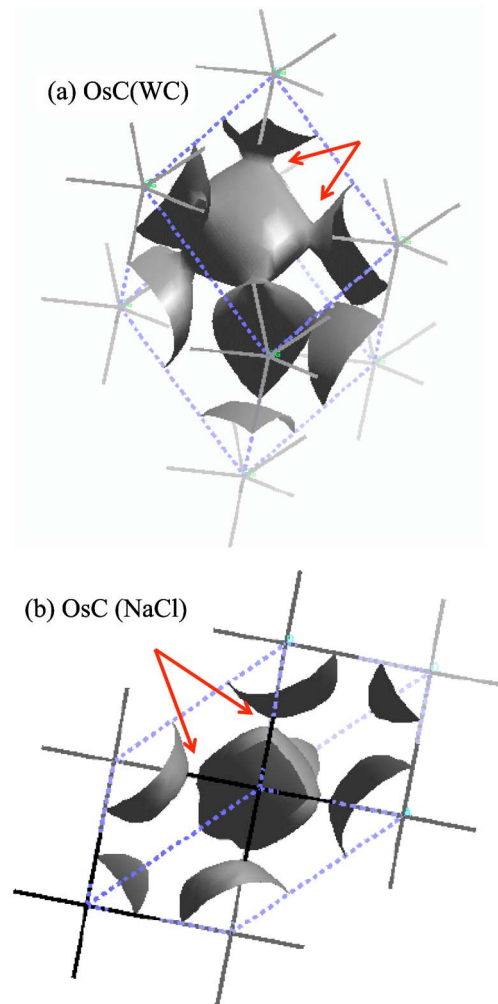


FIG. 4. (Color online) Charge density surfaces of OsC (WC) and OsC(NaCl). The charge value of the surface is chosen to be $0.7e$ per cell to distinguish the two structures. The unit cells are indicated by the dashed lines while the gray lines in the corners show the bondings to the atoms outside the unit cell. The arrows indicate the different charge distributions between Os-C in the hexagonal and cubic phases.

ume compression on directions (namely, c/a ratios) as a function of pressure for hexagonal Os, OsC, OsN, and OsO_2 (Fig. 2) shows the compressibility along c -axis is much lower than that along a -axis.

It is interesting to examine the relationship between electronic properties and mechanical properties (e.g., bulk modulus). According to Grossman *et al.*,⁵ the high bulk modulus of Os is attributed to its strong directional bonding. In comparison to the other sixth-row transition elements (W-Os), the directional bonding increases with the number of valence electrons. Similar trend is observed for the bulk modulus until it reaches the saturation of valence electron concentration in Os.⁵ However, in the osmium compounds, the directional bonds are changed to d - p hybridization in the presence of the C or N atoms. The bonding states in OsC and OsN are saturated and the antibonding states begin to be filled. Therefore, the bulk modulus decreases from Os to OsC and then to OsN. This picture can be seen clearly through the compari-

TABLE III. The expressions of the second order regression for the calculated c/a ratios: c/a (in Å) = $\lambda_0 + \lambda_1 P + \lambda_2 P^2$ (P is in GPa).

Systems	λ_0	$\lambda_1 (\times 10^{-4})$	$\lambda_2 (\times 10^{-7})$
Os(hex)	1.578	1.201	-4.212
OsC(WC) ^a	0.928	2.732	1.015
OsN(WC)	1.130	1.342	-5.191
OsO ₂ (rutile)	0.709	5.770	-14.91

^aLinear fit: $\lambda_0 = 0.928$, $\lambda_1 (\times 10^{-4}) = 2.829$.

son of density of states (DOS) of Os, OsC, and OsN in the hexagonal structures, as shown in Fig. 3, where the antibonding states are sharp and increase significantly from Os to OsC and OsN (as indicated by the arrows in Fig. 3).

We now turn to the comparison of bulk modulus of OsC in different structural phases. The charge density surfaces of OsC in the hexagonal and cubic structures are plotted in Fig. 4. The bonding of Os-C in OsC (WC) is stronger than that in OsC (NaCl), as indicated by the arrows in Fig. 4. Therefore the hexagonal OsC is less compressible than the cubic OsC. The same trend is observed for OsN.

The measured hcp c/a ratio of Os in high pressure XRD experiments has been shown to increase with applied pressure.⁶ This is confirmed by our first principles calculations, as shown in Fig. 2. Our calculations also find similar behavior for OsC and OsN in the WC structures as well as rutile OsO₂. Their calculated c/a ratios are slightly nonlin-

ear, except for OsC, which is linear. The expressions of the second order regression for the calculated c/a ratios are listed in Table III. We observe that keeping the c/a ratios fixed will result in different calculated values for bulk modulus. For example, when we used the same code with the ratios of c/a fixed while changing the volume, the value for Os (hcp) was 393 GPa. This value was underestimated compared to the value of 403 GPa, obtained by full relaxation using *ab initio* stress (by applying external static pressure).

In summary, first principles calculations have been performed to study the compressibility of Os, OsC, and OsN both in their cubic and hexagonal structural forms, and OsO₂ in its rutile structural form. Our calculated results suggest that both hexagonal and cubic Os are low-compressibility metals with bulk moduli of 403 and 401 GPa, respectively. Hexagonal Os, OsC, and OsN have lower compressibility than their cubic phases, as indicated from the calculated bulk moduli and equation of states. Among osmium's carbide, nitride and oxide, OsC in the WC structure is found to be least compressible with a bulk modulus of 396 GPa, suggesting that OsC has the potential to be a superhard compound for mechanical applications. The origin of high bulk modulus in Os and hexagonal OsC and OsN are explained in terms of electronic properties such as directional bonding, density of states, and charge density.

The author thanks Professor M. C. Payne and H. Q. Wang for fruitful discussions and Kai Loon Chen for proofreading the manuscript.

*Electronic address: jincheng.zheng@yahoo.com

- ¹H. J. McKimin and W. L. Bond, *Phys. Rev.* **105**, 116 (1957); I. V. Aleksandrov, A. F. Goncharov, A. N. Zisman, and S. M. Stishov, *Sov. Phys. JETP* **66**, 384 (1987); I. V. Aleksandrov, A. F. Goncharov, E. V. Yakovenko, and S. M. Stishov, *High Pressure Research: Application to Earth and Planetary Sciences*, edited by Y. Syono and M. H. Manghnani (TERRAPUB, Tokyo/American Geophysical Union, Washington, D.C., 1992), pp. 409–416.
- ²A. Y. Liu and M. L. Cohen, *Science* **245**, 841 (1989).
- ³C. S. Yoo, H. Cynn, F. Gygi, G. Galli, V. Iota, M. Nicol, S. Carlson, D. Häusermann, and C. Mailhot, *Phys. Rev. Lett.* **83**, 5527 (1999).
- ⁴L. S. Dubrovinsky, N. A. Dubrovinskaia, V. Swamy, J. Muscat, N. M. Harrison, R. Ahuja, B. Holm, and B. Johansson, *Nature (London)* **410**, 653 (2001); S. Desgreniers and K. Lagarec, *Phys. Rev. B* **59**, 8467 (1999).
- ⁵J. C. Grossman, A. Mizel, M. Cote, M. L. Cohen, and S. G. Louie, *Phys. Rev. B* **60**, 6343 (1999).
- ⁶H. Cynn, J. E. Klepeis, C. S. Yoo, and D. A. Young, *Phys. Rev. Lett.* **88**, 135701 (2002).
- ⁷F. Occelli, D. L. Farber, J. Badro, C. M. Aracne, D. M. Teter, M. Hanfland, B. Canny, and B. Couzinet, *Phys. Rev. Lett.* **93**, 095502 (2004).
- ⁸K. Takemura, *Phys. Rev. B* **70**, 012101 (2004).
- ⁹Accelrys Inc., *CASTEP Users Guide* (Accelrys Inc., San Diego, 2001); V. Milman, B. Winkler, J. A. White, C. J. Pickard, M. C. Payne, E. V. Akhmatkaya, and R. H. Nobes, *Int. J. Quantum Chem.* **77**, 895 (2000).
- ¹⁰M. C. Payne, M. P. Teter, D. C. Allan, T. A. Arias, and J. D. Joannopoulos, *Rev. Mod. Phys.* **64**, 1045 (1992).
- ¹¹P. Hohenberg and W. Kohn, *Phys. Rev.* **136**, B864 (1964); W. Kohn and L. J. Sham, *Phys. Rev.* **140**, A1133 (1965).
- ¹²J. P. Perdew and Y. Wang, *Phys. Rev. B* **45**, 13244 (1992).
- ¹³D. Vanderbilt, *Phys. Rev. B* **41**, R7892 (1990).
- ¹⁴H. J. Monkhorst and J. D. Pack, *Phys. Rev. B* **13**, 5188 (1976).
- ¹⁵L. Fast, J. M. Wills, B. Johansson, and O. Eriksson, *Phys. Rev. B* **51**, 17431 (1995).
- ¹⁶V. A. Finkel, M. I. Palatnik, and G. P. Kovtun, *Phys. Met. Metallogr.* **32**, 231 (1971).
- ¹⁷E. Knittle, R. B. Kaner, R. Jeanloz, and M. L. Cohen, *Phys. Rev. B* **51**, 12149 (1995), and references therein.
- ¹⁸*Landolt-Bornstein Tables (Landolt-Bornstein: Numerical Data and Functional Relationships in Science and Technology, New Series*, edited by O. Madelung (Springer, Berlin, 1982), Vol. 17a.
- ¹⁹J.-C. Zheng, C. H. A. Huan, A. T. S. Wee, R. Z. Wang, and Y. M. Zheng, *J. Phys.: Condens. Matter* **11**, 927 (1999); J.-C. Zheng, H. Q. Wang, C. H. A. Huan, and A. T. S. Wee, *ibid.* **13**, 5295 (2001).
- ²⁰H. Q. Wang, J. C. Zheng, A. T. S. Wee, and C. H. A. Huan, *J. Electron Spectrosc. Relat. Phenom.* **114**, 483 (2001).
- ²¹C. N. R. Rao and B. Raveau, *Transition Metal Oxides* (VCH, New York, 1995), p. 11.
- ²²E. Knittle, R. M. Wentzcovich, R. Jeanloz, and M. L. Cohen, *Nature (London)* **337**, 349 (1989).